HHS Public Access

Author manuscript

Hepatology. Author manuscript; available in PMC 2020 June 01.

Published in final edited form as:

Hepatology. 2019 June ; 69(6): 2562–2578. doi:10.1002/hep.30542.

Amelioration of Ductular Reaction by Stem Cell Derived Extracellular Vesicles in MDR2 Knockout Mice via Lethal-7 microRNA

Kelly McDaniel[1,2,*], **Nan Wu**[3,*], **Tianhao Zhou**[1,3,*], **Li Huang**[4], **Keisaku Sato**[3], **Julie Venter**[3], **Ludovica Ceci**[3], **Demeng Chen**[4], **Sugeily Ramos-Lorenzo**[1,2], **Pietro Invernizzi**[5], **Francesca Bernuzzi**[5], **Chaodong Wu**[6], **Heather Francis**[1,2,3], **Shannon Glaser**[2,3], **Gianfranco Alpini**[1,2,3], **Fanyin Meng**[1,2]

[1]Research Department, Central Texas Veterans Health Care System, Temple, TX

[2]Baylor Scott & White Digestive Disease Research Center, Baylor Scott & White Health, Temple, TX

[3]Department of Medical Physiology, Texas A&M University Health Science Center College of Medicine, Temple, TX

[4]Department of Pancreatobiliary Surgery and Center for Translational Medicine, the First Affiliated Hospital of Sun Yat-sen University, Guangzhou, China

[5]Center for Autoimmune Liver Diseases, Humanitas Clinical and Research Center, Rozzano, Italy

[6]Department of Nutrition and Food Science, Texas A&M University, College Station, TX.

Abstract

Cholangiopathies are diseases that affect cholangiocytes, the cells lining the biliary tract. Liver stem cells (LSCs) are able to differentiate into all cells of the liver and possibly influence the surrounding liver tissue by secretion of signaling molecules. One way in which cells can interact is through secretion of extracellular vesicles (EVs), which are small membrane-bound vesicles that contain proteins, microRNAs (miRNAs), and cytokines. We evaluated the contents of liver stem cell–derived EVs (LSCEVs), compared their miRNA contents to those of EVs isolated from hepatocytes, and evaluated the downstream targets of these miRNAs. We finally evaluated the crosstalk among LSCs, cholangiocytes, and human hepatic stellate cells (HSCs). We showed that LSCEVs were able to reduce ductular reaction and biliary fibrosis in multidrug resistance protein 2 $(MDR2)^{-/-}$ mice. Additionally, we showed that cholangiocyte growth was reduced and HSCs were deactivated in LSCEV-treated mice. Evaluation of LSCEV contents compared with EVs

ADDRESS CORRESPONDENCE AND REPRINT REQUESTS TO: Gianfranco Alpini, Ph.D., Richard L. Roudebush VA Medical Center, and Division of Gastroenterology & Hepatology, Department of Medicine, Indiana University, School of Medicine, 1481 W 10th street, Room C-7151, Indianapolis, IN 46202, galpini@iu.edu, Tel.: +1-317-988-2337; Fanyin Meng, Ph.D., Richard L. Roudebush VA Medical Center, and Division of Gastroenterology & Hepatology, Department of Medicine, Indiana University, School of Medicine, 1481 W 10th street, Room C-7153, Indianapolis, IN 46202, Mengf@iu.edu, Tel.: +1-317-988-2162.
*These authors contributed equally to this work.

Potential conflict of interest: Nothing to report.

Supporting Information

Additional Supporting Information may be found at onlinelibrary.wiley.com/doi/10.1002/hep.30542/suppinfo.

derived from hepatocytes showed a large increase in the miRNA, lethal-7 (let-7). Further evaluation of let-7 in MDR2$^{-/-}$ mice and human primary sclerosing cholangitis samples showed reduced levels of let-7 compared with controls. In liver tissues and isolated cholangiocytes, downstream targets of let-7 (identified by ingenuity pathway analysis), Lin28a (Lin28 homolog A), Lin28b (Lin28 homolog B), IL-13 (interleukin 13), NR1H4 (nuclear receptor subfamily 1 group H member 4) and NF-κB (nuclear factor kappa B), are elevated in MDR2$^{-/-}$ mice, but treatment with LSCEVs reduced levels of these mediators of ductular reaction and biliary fibrosis through the inhibition of NF-κB and IL-13 signaling pathways. Evaluation of crosstalk using cholangiocyte supernatants from LSCEV-treated cells on cultured HSCs showed that HSCs had reduced levels of fibrosis and increased senescence.

Conclusion: Our studies indicate that LSCEVs could be a possible treatment for cholangiopathies or could be used for target validation for future therapies.

Cholangiopathies are diseases that affect the biliary epithelium and lead to fibrotic scarring. Primary sclerosing cholangitis (PSC) primarily affects middle-age men and is thought to be an inflammatory autoimmune disease targeting cholangiocytes.[1] The chronic inflammation involved in PSC leads to destruction of the bile ducts, causing blockage of bile ducts and fibrotic scarring, eventually culminating in cirrhosis and liver failure.

The MDR2$^{-/-}$ mouse is a commonly used mouse model of PSC. The MDR2$^{-/-}$ mouse has a mutation in the *ABCB4* gene, the gene for multidrug resistance protein 2 (MDR2), which prevents the mice from secreting phospholipids into the bile.[2] This causes the bile to become corrosive, destroying cholangiocytes, which leads to a histological appearance very similar to PSC patients. Cholestatic liver injury induces cholangiocytes to proliferate, which results in ductular reaction, portal fibrosis, and biliary cirrhosis.[3] Therefore, blockage of cholangiocyte proliferation could be a mechanism by which PSC-induced fibrosis could be ameliorated. We have previously shown that prolonged exposure to darkness, melatonin administration, or treatment with gonadotropin-releasing hormone is able to ameliorate the fibrotic scarring seen in the MDR2$^{-/-}$ mouse.[4,5]

Stem cell therapy is a novel treatment paradigm that has been pursued more in the past few years in both basic science and in the clinic. This treatment is being used to regenerate tissues after disease in neurological and cardiac diseases as well as osteoarthritis.[6-8] We have previously shown that small cholangiocytes, which may contain a subpopulation of biliary progenitor cells, reduced fibrotic scarring in bile duct ligation (BDL) mice through activation of forkhead box A2 (FoxA2).[9]

MicroRNAs (miRNAs) are small noncoding RNAs that can regulate gene expression through direct binding to mRNA or DNA. Several miRNAs are altered in liver diseases, including lethal-7 (let-7). The miRNA let-7 is reduced in MDR2$^{-/-}$ mice, PSC patients, and cholestatic liver patients.[10] We have previously shown that suppression of Lin28 homolog, a downstream target of let-7, increases let-7 and mitigates progression of alcoholic liver disease.[11] Additionally, we have shown that increased let-7 expression as a result of suppression of secretin ameliorated cholestatic liver injury.[10] Let-7, as well as other miRNAs, could be transmitted from stem cells to damaged cells through extracellular

vesicles (EVs) to repair or ameliorate damage during liver repair through their downstream targets.

EVs are secreted by cells to communicate with other cells at local or distant locations.[12,13] They are typically 30-800 nm in size, consisting of exosomes, microvesicles and apoptotic bodies, and have been shown to be important in many disease states.[14,15] EVs could possibly be important in biliary disorders due to interactions between cholangiocytes and their surrounding tissues. It has been shown that cholangiocytes secrete EVs into the bile duct lumen, which can interact with cilia of other cholangiocytes.[16] We have previously shown that cholangiocytes interact through EVs as a result of cellular injury.[17] Although it is a novel area, EVs could be used as a therapeutic tool in cholestatic liver injury. Recently, cross-sectional analyses at the time of initial liver biopsy in patients with chronic hepatitis C showed that reduced levels of let-7a/7c/7d-5p (let-7s) in plasma and EVs were correlated with advanced histological hepatic fibrosis stage and other fibrotic markers.[18] Another study showed that miRNA-containing circulation EVs could be used to positively identify and differentiate among PSC, hepatocellular carcinoma, and cholangiocarcinoma.[19]

PSC currently has very few treatment options and patient outcome is dismal. An option for this type of degenerative disease could be to aid the liver in repairing itself. Because stem cells have been successful in other diseases, stem cell therapy could be a possible treatment option. EVs derived from liver stem cells should be ideal to aid the liver in repairing itself after cholestatic injury. This study aims to evaluate the ability of stem cell-derived EVs to ameliorate cholestatic liver injury in a mouse model of PSC.

Methods and Materials

MATERIALS

Reagents were purchased from Sigma-Aldrich (St. Louis, MO) unless otherwise indicated. The mouse and human PCR primers were purchased from Qiagen (Valencia, CA) and are listed in Supporting Table S1. The microRNA primers were purchased from Thermo Fisher Scientific (Waltham, MA). The primary antibodies for cytokeratin-19 (CK-19), albumin, interleukin 13 (IL-13), alpha fetoprotein (AFP), nuclear factor kappa B (NF-κB) 1, nuclear factor of kappa light polypeptide gene enhancer in B cells inhibitor alpha (IκBα), collagen1A1 (Col1A1), and desmin were purchased from Abcam (Cambridge, MA).

HUMAN SUBJECTS

Human samples were obtained from Dr. Pietro Invernizzi (Liver Unit and Center for Autoimmune Liver Diseases, Humanitas Clinical and Research Center, Rozzano, Milan, Italy) under a protocol by the Ethics Committee of the Humanitas Research Hospital; the protocol was also reviewed by the Veterans' Administration internal review board and International Research Committee. The use of human tissue was also approved by the Texas A&M Health Science Center College of Medicine Institutional Review Board. Formalin-fixed, paraffin-embedded liver sections (4-5-mm thick) were obtained from 3 patients with PSC, 3 control healthy livers were obtained from patients undergoing resection of liver

metastasis, and total RNA was isolated for real-time quantitative PCR as described (please see our previous publication for patient information[9]).

ANIMAL MODELS

The Animal Care and Use Committee of Baylor Scott & White approved all of the animal protocols used in the study. Female MDR2$^{-/-}$ (FVB.129P2-Abcb4^{tm1Bor}/J) mice and wild-type (WT, FVB/NJ) controls (27 weeks of age) were originally obtained from Jackson Laboratories (Bar Harbor, ME) and subsequently bred in-house. Liver stem cell (LSC)–derived EVs (LSCEVs) were injected intravenously at 4.6×10^7 particles per injection through the lateral tail vein once per week for 2 weeks. Mice were sacrificed and livers were collected 2 weeks later (29 weeks of age).

CELL LINES

The immortalized normal human cholangiocyte cell line, H69, was a gift from Dr. G.J. Gores, Mayo Clinic, Rochester, MN. Immortalized murine normal pooled cholangiocyte lines were also used.[10] Human LSCs were purchased from Creative Bioarray (Shirley, NY). The human hepatic stellate cells,[20] human mesenchymal stem cells (MSCs) and human hepatocytes (HHs) were purchased from Sciencell (Carlsbad, CA). The human acute monocytic leukemia cell line (THP-1) was purchased from ATCC Inc. (Manassas, VA) and maintained in Roswell Park Memorial Institute 1640 medium (Sigma-Aldrich) with 10% fetal calf serum (FCS) without antibiotics.

ISOLATION OF HUMAN AND MOUSE CHOLANGIOCYTES BY LASER CAPTURE MICRODISSECTION IN THE AREAS OF DUCTULAR REACTION

Human and mouse cholangiocytes as well as mouse hepatocytes (200 cells) were isolated by laser capture microdissection (LCM) in or near the area of ductular reaction as described[9] (using CK-19 as a marker of cholangiocytes and albumin as the marker of mature hepatocytes). The RNA from LCM-isolated human and mouse cholangiocytes/hepatocytes were extracted with the Arcturus PicoPure RNA isolation kit (Thermo Fisher Scientific, Mountain View, CA) according to the instructions provided by the vendor. The expression of let-7a, let-7c, IL-13, NR1H4 (nuclear receptor subfamily 1 group H member 4), NF-κB, FoxA2, and IκBα was measured in these cells by Taqman miRNA PCR assay or real-time quantitative PCR. All studies were performed in quadruplicate unless otherwise specified.

SUPERARRAY QUANTITATIVE PCR ASSAY AND REAL-TIME QUANTITATIVE PCR ANALYSIS

RNA was isolated from liver tissues or cell lysates using TRIzol (Invitrogen) according to the manufacturer's protocol. The RNA was subsequently cleaned using the RNeasy Kit (Qiagen) according to the manufacturer's protocol.

STATISTICS

Data are expressed as the mean ± SEM from at least three separate experiments performed in triplicate unless otherwise noted. The differences among groups were analyzed using a double-sided Student *t* test when only two groups were present and analysis of variance

when there were more than two groups. The null hypothesis was rejected at the 0.05 level unless otherwise specified.

Please see the Supporting Information for more detailed information.

Results

CHARACTERIZATION OF HUMAN LSCs AND LSCEVs

Before extraction of EVs, we verified the state of our stem cell culture by immunofluorescence for specific hepatic stem cell markers. Immunofluorescence of LSCs for the hepatic stem cell markers CK-18, epithelial cell adhesion molecule (EpCam), and AFP showed that these markers were all highly expressed in LSCs, indicating that these cells exhibit properties of hepatic stem cells (Fig. 1A). We then evaluated LSCs for their ability to excrete EVs, as well as the quality of our LSCEV preparation by transmission electron microscopy (TEM). TEM revealed LSC excretion of multiple-sized EVs into the surrounding media (Fig. 1B, upper panels). The presence of EVs in our preparation was verified with TEM, showing that there were EVs less than 500 nm in our preparation that appear to be about 300 nm and smaller (Fig. 1B, lower panels).

To evaluate the amount and size distribution of our EVs, we used a NanoSight (Salisbury, United Kingdom) nanoparticle imaging system to analyze our EV preparation. Analysis of our preparation revealed that most of our LSC-isolated EVs were approximately 110-350 nm (Fig. 1C). Following quantification, our preparation had a concentration of 12.09 particles per frame, which equated to a concentration of 1.39×10^8 particles/mL.

INCORPORATION OF HUMAN LSCEVs IN H69 HUMAN CELL LINES

LSCEVs labeled with PKH26 green dye were incorporated by cultured H69 human cholangiocytes as shown by confocal microscopy (Fig. 1D). EV treatment with soluble hyaluronic acid and anti-CD44 blocking antibodies inhibited EV incorporation in H69 cells (Fig. 1E), suggesting that expression of CD44 is critical for their internalization. Moreover, removal of surface molecules by trypsin treatment of EVs inhibited their incorporation in H69 cells, confirming the relevance of surface molecules in EV internalization. Additionally, we confirmed that LSCEVs labeled with PKH26 dye were incorporated by cultured normal HHs (Supporting Fig. S1).

IN VITRO PROLIFERATIVE AND APOPTOTIC/FIBROSIS REGULATION EFFECTS OF HUMAN LSCEVs

Incubation of H69 cells with different doses of LSCEVs promoted normal cell proliferation under serum deprivation conditions compared with control cells incubated with EVs extracted from human hepatocytes (HHEVs) (Fig. 2A), but significantly blocked lipopolysaccharide (LPS)-induced cell proliferation in a dose-dependent manner (Fig. 2B), suggested the dual effects of LSCEVs on cell proliferation in normal and inflammatory conditions. Additionally, LSCEVs induced synthesis of hepatocyte growth factor and stem cell factor (Fig. 2C). Furthermore, incubation of H69 cells with LSCEVs significantly inhibited apoptosis in human cholangiocytes induced by tumor necrosis factor α (TNF-α)

(Fig. 2D). Treatment of human cholangiocytes with transforming growth factor beta (TGF-β 10 mM, 72 hours) significantly increased fibrosis marker α-smooth muscle actin (α-SMA) mRNA expression by 90% of control (H69-EV treated) human cholangiocytes (Fig. 2E). In addition, LSCEV treatment reduced TGF-β-induced fibrotic response, with almost 40% prevention of α-SMA mRNA expression at 30 μg/mL. Furthermore, the cellular senescence index in TGF-β-treated human hepatic stellate cells (HSCs) was increased to 255.4% of the control by a 48-hour LSCEV treatment (Fig. 2F). Thus, both the protective effects of LSCEV against LPS-induced ductular reaction and TGF-β-induced fibrosis in cholangiocytes, plus the activation in HSCs, might contribute to its recovery activity.

MEASUREMENT OF LIVER HISTOLOGY AND FIBROSIS AND DUCTULAR REACTION IN MDR2$^{-/-}$ MICE TREATED WITH LSCEVs

Because LSCs are often not close to their targets and may communicate through EVs, we hypothesized that LSCEVs could possibly aid in liver repair after injury. Hematoxylin and eosin staining showed altered liver structure and inflammatory infiltration in MDR2$^{-/-}$ mice compared with WT mice (Fig. 3A). Administration of LSCEVs reduced the amount of inflammatory infiltration and structural damage seen in the MDR2$^{-/-}$ mice (Fig. 3A).

Sirius red staining of livers for collagen deposition showed a large increase in collagen staining in MDR2$^{-/-}$ mice compared with WT counterparts, indicating a large increase in fibrotic scarring in MDR2$^{-/-}$ mice (Fig. 3B). Two treatments of intravenous LSCEVs reduced sirius red staining, indicating less liver fibrosis. Quantification of collagen deposition showed a significant increase in collagen in MDR2$^{-/-}$ mice, which was significantly reduced following treatment with LSCEVs (Fig. 3C). Additionally, Col1A1 and alpha smooth muscle actin (ACTA2) expression was decreased in total liver and isolated cholangiocytes from LSCEV-treated MDR2$^{-/-}$ compared with control-treated MDR2$^{-/-}$ mice (Fig. 3D). Taken together, these data indicate that LSCEVs reduce fibrosis in MDR2$^{-/-}$ most likely by halting further progression of the disease, but possibly repairing the damage that had already occurred.

Ductular reaction is a vital component of cholangiopathies and is thought to be a compensatory mechanism during the damage of bile ducts.[21] CK-19 staining for cholangiocytes shows increased ductular reaction in MDR2$^{-/-}$ control mice that was decreased in MDR2$^{-/-}$ mice treated with LSCEVs (Fig. 4A). Quantification of ductular reaction showed that MDR2$^{-/-}$ mice have significantly intrahepatic bile duct mass (IBDM), which was attenuated in LSCEV-treated MDR2$^{-/-}$ mice (Fig. 4A). Enhanced macrophage infiltration was observed in the areas of ductular reaction in MDR2$^{-/-}$ mice liver by double-staining immunohistochemistry, and significantly reduced after LSCEV treatment (Fig. 4B). Along with the ductular reaction, fibrosis marker α-SMA was also significantly increased near CK-19-positive IBDM, which was also attenuated after LSEV treatment in MDR2$^{-/-}$ mice liver (Fig. 4C). To further evaluate the status of cholangiocytes, we measured the expression of the proliferative markers, Ki-67 and proliferating cell nuclear antigen (PCNA). Both Ki-67 and PCNA were increased in isolated cholangiocytes from MDR2$^{-/-}$ compared with WT mice, but these markers were both reduced in LSCEV-treated mice (Fig. 4D).

Because cellular senescence is important to the health of the liver, and the acquisition of a senescence-associated secretory phenotype relates to the changes in ductular reaction, we measured cellular senescence in isolated cholangiocytes by real-time quantitative PCR for the senescence markers p16 and p21. Overall senescence was increased in MDR2$^{-/-}$ total liver isolates due to the rapid cholangiocyte turnover caused by the ductular reaction, but attenuated in LSCEV-treated total liver isolates (Fig. 4E).

IDENTIFICATION OF MIRNAs INVOLVED IN LSCEV-MODULATED LIVER REPAIR DURING CHRONIC BILIARY INJURY

To evaluate the contents of LSCEVs compared with EVs extracted from HHEVs, RNA was extracted from isolated LSCEVs and HHEVs and analyzed with a microRNA PCR array. When the results of the arrays were analyzed with the manufacturer's software, we found that compared with HHEVs, LSCEVs had increased levels of several miRNAs, including let-7a, let-7b, and miR-25 (Fig. 5A). We have previously shown let-7a to be an important factor in the repair of liver injury; therefore, we selected let-7a to analyze further in our model.[11]

ANALYSIS OF LIVER REPAIR MECHANISMS IN MDR2$^{-/-}$ MICE TREATED WITH LSCEVs

To analyze the effectiveness of LSCEVs, which contain let-7a, we analyzed the downstream targets of let-7, Lin28 homolog A (Lin28a), and Lin28 homolog B (Lin28b). Real-time quantitative PCR for Lin28a and Lin28b in total liver isolates showed that both Lin28a and Lin28b expression is increased in MDR2$^{-/-}$ mice (Fig. 5B). Treatment with LSCEVs reduced both Lin28a and Lin28b expression in total liver isolates from MDR2$^{-/-}$ mice. In isolated cholangiocytes, only Lin28a was elevated in MDR2$^{-/-}$ mice, and treatment with LSCEVs reduces Lin28a levels in cholangiocytes compared with normal levels (Fig. 5C). This indicates that Lin28b levels are controlled by noncholangiocyte cells in the liver, most likely hepatocytes, whereas Lin28a levels are more important in cholangiocytes.

We have previously shown that small cholangiocyte treatment ameliorates liver injury in MDR2$^{-/-}$ mice through enhanced expression of FoxA2.[4] Therefore, to evaluate liver repair in these mice, we evaluated FoxA2 expression in liver sections. Staining for FoxA2 showed diminished levels of FoxA2 in the cholangiocytes of MDR2$^{-/-}$ mice, but treatment with LSCEVs restored FoxA2 levels in cholangiocytes (Fig. 5D). Real-time quantitative PCR in total liver isolates showed that FoxA2 levels are decreased in MDR2$^{-/-}$ mice, and treatment with LSCEVs increases FoxA2 levels in MDR2$^{-/-}$ mice (Fig. 5E). In isolated cholangiocytes, FoxA2 was suppressed in MDR2$^{-/-}$ mice, but treatment with LSCEVs begins to restore FoxA2 levels to normal levels (Fig. 5F).

LET-7 BLOCKS NF-KB ACTIVATION IN LPS-STIMULATED H69 CELLS AND MDR2$^{-/-}$ MICE LIVER

Ingenuity pathway analysis (IPA) was performed based on the data from PCR array and LSCEVs treated MDR2$^{-/-}$ mice to determine the cellular context of the differentially expressed let-7 signaling mechanisms related to the recovery of cholestatic liver injury. IPA analysis indicated that IL-13 and NR1H4 are the key mediators in the inflammatory/fibrotic

responses associated with let-7 signaling, whereas NF-κB is critical in the antiductular reaction effects of let-7 (Fig. 6A).

To further advance mechanistic insights into the role of let-7 in ductular reaction, including its effects on cytokines and the NF-κB signaling pathway, we assessed the gene-expression profile of LPS-treated H69 cells with let-7 modulation. We performed a Human Chemokines & Receptors PCR Array (selected based on IPA with the focus of NF-κB signaling-associated gene list) to identify let-7 target genes in LPS-treated Pre-let-7a-transfected H69 cells compared with LPS-treated Pre-miRNA control (Pre-miRNA-Con)–transfected H69 cells (Fig. 6B, left). Of the 84 NF-κB-signaling pathway–associated genes, six genes (7.1%) were up-regulated by 2-fold or greater in Pre-let-7a-transfected H69 cells compared with Pre-miRNA-Con-transfected H69 cells in the presence of LPS stimulation, and only one gene (1.2%) (IκBα) was up-regulated by 2-fold or greater with $P < 0.05$ in Pre-let-7a-transfected H69 cells compared with Pre-miRNA-Con-transfected H69 cells in the presence of LPS stimulation (Fig. 6B, right; n = 4, $P < 0.05$). The inhibition of several key mediators of NF-κB pathway, such as IL-13 and NF-κB1, were observed based on the PCR array data (Fig. 6B). To confirm the functional effect and relevance of LSCEV/let-7-dependent modulation of IL-13, NF-κB, and NR1H4 in the ductular reaction areas of PSC animal and patients' liver *in vivo*, we assessed the mRNA expressions of let-7a, let-7c, IL-13, NF-κB1, IκBα, and NR1H4 in isolated cholangiocytes by LCM. The mRNA expressions of IL-13, NF-κB1, and NR1H4 were significantly increased in LCM-isolated cholangiocytes from the ductular reaction fields of PSC patients/MDR2$^{-/-}$ mice liver when compared with healthy/WT controls, along with the significant reductions of let-7a, let-7c, and IκBα (Fig. 6C,D). Real-time quantitative PCR assay has also confirmed the recovery effects by LSCEV treatment to partially inhibit NF-κB/IL-13 activation through let-7 in cholangiocytes isolated from ductular reaction fields by LCM (Fig. 6C). Double-staining immunohistochemistry analyses have confirmed the enhanced IκBα phosphorylation (Fig. 6E, top) and degradation (Fig. 6E, bottom) as well as increased IL-13 expression (Fig. 6F, top) and NF-κB (p65 subunit) translocation (Fig. 6F, bottom) in ductular reaction fields in MDR2$^{-/-}$ mice liver, and the recovery effects by LSEV treatment to partially inhibit the cholangiocytes' NF-κB/IL-13 activation (Fig. 6E,F). Meanwhile, only moderate changes with the insignificant trend were observed in LCM-isolated hepatocytes (albumin^{+}) from LSCEV-treated mice liver (Supporting Fig. S2).

LET-7 INHIBITS CYTOKINE PRODUCTION AND FIBROTIC RESPONSE IN H69 CELLS

We then examined whether let-7 could inhibit the production of inflammatory cytokines and fibrotic responses induced by TGF-β in H69 cells. IL-13, α-SMA, and Col1A1 mRNA expression levels in TGF-β-treated H69 cells transfected with Pre-let-7a were significantly inhibited, compared with those in TGF-β-treated H69 cells transfected with Pre-miRNA-Con (Fig. 7A). The modulation of IL-13 by let-7a in conditioned medium was also verified by enzyme-linked immunosorbent assay (Fig. 7B). Our results demonstrated that IL-13 was reduced in conditioned medium from the let-7a-transfected H69 cells after TGF-β stimulation compared with control. Meanwhile, overexpression of let-7a significantly increased FoxA2 mRNA expression in cultured H69 cells (Supporting Fig. S3). We also investigated the regulation effects of NF-κB and farnesoid X receptor signaling by let-7 in

TGF-β-treated normal HHs and observed only a slight trend toward significance (Supporting Fig. S4).

CONDITIONED MEDIA FROM LET-7-TRANSFECTED H69 CELLS SUPPRESS HUMAN MONOCYTE-DERIVED THP-1 CELL AND HUMAN HSC MIGRATION

We then examined the functional role of the let-7-mediated inhibition of inflammatory cytokine expression and fibrotic response. We performed *in vitro* migration assays to determine whether conditioned media from let-7-transfected H69 cells could suppress the migration of THP-1 cells and HSCs. For this experiment, conditioned media from H69 cells transfected with Pre-let-7a or control Pre-miRNA were evaluated. The migration of THP-1 cells and HSCs were markedly decreased (about 68% for THP-1 and 45% for HSC, respectively) when conditioned media from H69 cells transfected with Pre-let-7a was used. The number of migrated THP-1 cells was 32,500,500/well, 38,000/well, or 26,600/well when conditioned medium from H69 cells transfected with mock, Pre-miRNA-Con or Pre-let-7a, respectively, was used. The fluorescence intensity of migrated HSCs presented similar change patterns as THP-1 cells (Fig. 7C). These data suggest that the inhibition of inflammatory cytokine production and fibrotic response together with let-7 in cholangiocytes inhibits the migration of monocytes and monocyte-derived cells as well as HSCs, supporting the concept that let-7 prevents hepatic inflammation and fibrosis by inhibiting cytokine production and the recruitment of immune cells to the liver.

IN VITRO ANALYSIS OF THE INTERACTION OF STELLATE CELLS AND CHOLANGIOCYTES DURING LIVER INJURY

To ascertain the communication among stem cells, cholangiocytes, and HSCs in the regulation of liver fibrosis, stem cell-derived EVs were used to treat H69 cells (nonmalignant cholangiocytes) for 48 hours. The media on the H69 cells was changed to serum-free media and allowed to incubate for 48 hours and then transferred to HSCs for 48 hours. HSCs were then analyzed for fibrosis and senescence.

HSCs treated with media from H69 cells previously treated with LSCEVs showed a decrease in α-SMA (Fig. 7D). This indicates that the cells may in fact be deactivated. Because senescence has been shown previously to be important in the deactivation of HSCs during liver injury, we also measured the senescence of these cells to determine their activation level.[9] When HSCs were treated with media from H69 cells treated with LSCEVs, there was a significant increase in senescence as measured with the mRNA level of p16 (Fig. 7E), the senescence and deactivation marker of HSC. Interestingly, the mRNA expressions of platelet-derived growth factor and insulin-like growth factor 1, two major activators of HSCs, were significantly reduced in LSCEV-treated H69 cells with or without TGF-β stimulation relative to the controls (Supporting Fig. S5).

Discussion

The major findings in this study indicate that LSCs are able to communicate to cholangiocytes and stellate cells through EVs containing let-7, which are able to reduce overall liver damage (Fig. 8). We have shown that LSCs are able to release EVs and these

EVs average approximately 200 nm. Injection of LSCEVs into MDR2$^{-/-}$ mice reduced inflammation, fibrosis, ductular reaction, and liver fibrosis. Compared with hepatocyte-derived EVs, LSCEVs contain elevated levels of let-7 family members. Downstream targets of let-7, Lin28a, Lin28b, IL-13, NR1H4, and NF-κB1 were reduced in liver tissues and isolated cholangiocytes from LSCEV-treated MDR2$^{-/-}$ mice compared with MDR2$^{-/-}$ mice. Additionally, FoxA2 levels, a marker of repair, were restored in MDR2$^{-/-}$ mice treated with LSCEVs. We further investigated the interplay of signals by treating cholangiocytes with LSCEVs and then treated HSCs with the media from these cells. This showed that LSCEVs altered the signaling in cholangiocytes, which altered their secretion of cytokines or EVs, which reduced ductular reaction and biliary fibrosis but increased senescence in HSCs.

There are several locations of presumptive stem cell populations in the liver. HSCs (oval cells) are located in the canals of Hering and are able to differentiate into mature cholangiocytes or hepatocytes.[22] Biliary stem/progenitor cells are thought to be located in the small cholangiocyte population as well as in the peribiliary glands.[4,23] We have shown previously that treatment with progenitor cells located in the small cholangiocyte population is able to ameliorate the damage caused by bile duct ligation via activation of FoxA2. Additionally, the biliary progenitor cells that reside in the small cholangiocyte population were able to deactivate HSCs by reduction of fibrotic markers and enhancement of senescence.[4] Interestingly, supernatants, which most likely contain EVs, from isolated small cholangiocytes of these mice were able to suppress fibrogenic markers and enhance senescence markers in cultured stellate cells, indicating that crosstalk between cholangiocytes and stellate cells is possible during liver repair.[4]

EVs are a mechanism by which cells can communicate with one another, and EV secretion may be elevated during liver injury. Recently, many studies have been performed with stem cell–derived EVs and liver injury. EVs derived from mesenchymal stem cells (MSCEVs) have been shown to improve the survival of mice with d-galactosamine/TNF-α-induced lethal hepatic failure.[24] MSCEVs have also been shown to be a protective treatment when administered before ischemic-reperfusion liver injury in mice.[25] Additionally, MSCEVs that contained the miRNA miR-223 have been shown to have a protective effect in an experimental hepatitis mouse model as well.[26] LSCEVs have not been used in an *in vivo* model of liver injury before our study. Recently, a mouse model of *ex vivo* normothermic machine perfusion (NMP) was used to test the ability of LSCEVs to protect against to ischemic-reperfusion liver injury, and it was shown that LSCEVs were able to reduce liver injury during hypoxic NMP. Overall, MCSEVs or LSCEVs have been shown to be protective against ischemia-reperfusion injuries as well as hepatic failure and hepatitis. Our study examines LSCEVs in a model of cholangitis. The ability of LSCEVs to ameliorate the damage caused by cholestatic liver injury is an important step forward in the treatment of cholestasis.

It has been shown that the levels of several miRNAs, including let-7a, in exosome-rich fractionated serum in patients with chronic liver disorders were correlated with the histological grade of hepatic fibrosis using microarray.[27] Circulating let-7 expression levels in plasma and EVs, as measured by comprehensive microarray and real-time quantitative PCR, were inversely correlated with the severity of hepatic fibrosis.[18] Up to 90% of

circulating miRNAs are associated with proteins, and different miRNAs were enriched in specific extracellular compartments (e.g., let-7a was predominant in the vesicle-rich fractions in healthy individuals[28]). We have demonstrated that let-7 regulates liver inflammation and fibrosis through lin28.[11] In PSC models we have alternatively shown that an increase of let-7, by repression of Lin28, improved fibrosis after alcoholic liver injury and decreased tissue inhibitor of metalloproteinase 3 levels. Meanwhile, LIN28 also functions as a bipartite RNA-binding protein that posttranscriptionally inhibits the biogenesis of let-7 microRNAs to regulate development and influence disease states.[29] Up-regulation of let-7 in the alcoholic liver disease model was able to modulate fibrosis by enhancing senesce in HSCs, which in turn reduced fibrosis.[11] Let-7 has also been demonstrated to directly target IL-13, a critical mediator of ductular reaction, steatohepatitis, and liver fibrosis.[30,31] IL-13 can promote fibrosis through both TGF-β-dependent and independent mechanisms.[32] NR1H4 modulates cholestasis by controlling bile acids and is involved in bile acid synthesis, bile excretion, and serum export. NR1H4 knockout mice have been shown to be protected from obstructive cholestasis.[33] From these data, it would be expected that enhancement of let-7 would promote liver repair and health. This expectation is realized when enhancement of let-7 by let-7-containing LSCEVs is able to repair the cholestatic liver damage seen in $MDR2^{-/-}$ mice.

We have shown in several studies that cholangiocytes and HSCs interact to regulate fibrosis during cholestatic liver disease. Because cholangiocytes are the target of cholestatic liver disease, they are the first to signal distress to the rest of the liver through release of various molecules, including secretin, histamine, vascular endothelial growth factor, progesterone, and serotonin.[34] As stated previously, we showed that treatment with small cholangiocytes in BDL mice was able to deactivate HSCs and reduce fibrosis and liver injury.[4] In another study, it was shown that knockout of miR-21 which is up-regulated in cholangiocytes, was able to reduce fibrosis and inhibit HSC activation in BDL mice.[35] We also showed that cholangiocyte supernatants can regulate fibrotic and senescence gene expression in cultured HSCs, solidifying the capability of cholangiocytes and HSCs to interact.[4] When looking at the actions of LSCEVs in this study, it is logical to think that the cholangiocytes, being the target of the initial damage, would be a target of the LSCEVs. Because the LSCEVs were injected through the tail vein and most likely to pass HSCs before cholangiocytes, it is not surprising that they are able to affect HSCs. However, more than likely, cholangiocytes secrete their own EVs to influence HSCs after they have interacted with LSCEVs. We demonstrated this in our final experiment of this study by treating HSCs in culture with supernatants of intramyocellular lipids treated with LSCEVs. The reduction in fibrosis and increase in senescence seen in the HSCs clearly shows that this interaction is likely.

In conclusion, we have shown that LSCEVs are able to reduce ductular reaction and biliary fibrosis in $MDR2^{-/-}$ mice through let-7-dependent reduction of Lin28a, Lin28b, IL-13, NF-κB, and NR1H4, and enhancement of FoxA2 (Fig. 8). Overall, LSCEV treatment could be pursued further to validate let-7 as a target or to use LSCEVs themselves as a treatment for cholestatic liver disease.

Supplementary Material

Refer to Web version on PubMed Central for supplementary material.

Acknowledgments:

This material is the result of work supported by resources at the Central Texas Veterans Health Care System. The views expressed in this article are those of the authors and do not necessarily represent the views of the Department of Veterans Affairs.

Supported by the Dr. Nicholas C. Hightower Centennial Chair of Gastroenterology from Baylor Scott & White; a VA Research Career Scientist Award; VA Merit Awards from the United States Department of Veteran's affairs, Biomedical Laboratory Research and Development Service (5I01BX000574 to G.A.; 5I01 BX001724 to F.M.; 1I01BX003031 to H.F.); NIH National Institute of Diabetes and Digestive Kidney Diseases (R01DK95862 to C. W., and 1R01DK108959 to H.F.); NIH (DK058411, DK076898, DK115184, DK110035, AA025997, and AA 025157 to G.A., F.M., and S.G.), and PSC Partners Seeking a Cure and Strategic Research Initiative (SRI) grant 41-855-96 by Indiana University Health.

Abbreviations:

ACTA2	alpha smooth muscle actin
BDL	bile duct ligation
CK	cytokeratin
Col1A1	collagen type 1 alpha 1
Con	control
EV	extracellular vesicle
FCS	fetal calf serum
FoxA2	forkhead box A2
HH	human hepatocyte
HHEV	human hepatocyte–derived EV
HSC	hepatic stellate cell
IL-13	interleukin 13
IκBα	nuclear factor of kappa light polypeptide gene enhancer in B cells inhibitor alpha
IPA	ingenuity pathway analysis
LCM	laser capture microdissection
let-7	lethal-7
Lin28a	Lin28 homolog A
Lin28b	Lin28 homolog B

LPS	lipopolysaccharide
LSC	liver stem cell
LSCEV	LSC-derived EV
MDR2	multidrug resistance protein 2 (encoded by the ABCB4 gene)
miRNA	microRNA
MSC	mesenchymal stem cell
MSCEV	mesenchymal stem cell–derived EV
NF-κB	nuclear factor kappa B
NR1H4	nuclear receptor subfamily 1 group H member 4
PCNA	proliferating cell nuclear antigen
PSC	primary sclerosing cholangitis
TEM	transmission electron microscopy
TGF-β	transforming growth factor beta
THP-1	human acute monocytic leukemia cell line
TNF-α	tumor necrosis factor α
WT	wild type
α-SMA	α-smooth muscle actin

REFERENCES

1). Eaton JE, Talwalkar JA, Lazaridis KN, Gores GJ, Lindor KD. Pathogenesis of primary sclerosing cholangitis and advances in diagnosis and management. Gastroenterology 2013;145:521–536. [PubMed: 23827861]

2). Smit JJ, Schinkel AH, Oude Elferink RP, Groen AK, Wagenaar E, van Deemter L, et al. Homozygous disruption of the murine mdr2 P-glycoprotein gene leads to a complete absence of phospholipid from bile and to liver disease. Cell 1993;75:451–462. [PubMed: 8106172]

3). Roskams T, Desmet V. Ductular reaction and its diagnostic significance. Semin Diagn Pathol 1998;15:259–269. [PubMed: 9845427]

4). Kyritsi K, Meng F, Zhou T, Wu N, Venter J, Francis H, et al. Knockdown of hepatic gonadotropin-releasing hormone by vivo-morpholino decreases liver fibrosis in multidrug resistance gene 2 knockout mice by down-regulation of miR-200b. Am J Pathol 2017;187:1551–1565. [PubMed: 28502477]

5). Wu N, Meng F, Zhou T, Han Y, Kennedy L, Venter J, et al. Prolonged darkness reduces liver fibrosis in a mouse model of primary sclerosing cholangitis by miR-200b down-regulation. FASEB J 2017;31:4305–4324. [PubMed: 28634212]

6). Zheng Y, Huang C, Liu F, Lin H, Niu Y, Yang X, et al. Reactivation of denervated Schwann cells by neurons induced from bone marrow-derived mesenchymal stem cells. Brain Res Bull 2018;139:211–223. [PubMed: 29524470]

7). Yang M, Xu Q, Liu B, Chen X, Li Y. Methodological exploration of bone marrow stem cell therapy in acute myocardial infarction—how to achieve greater benefit on cardiac outcomes: a systematic review and meta-analysis. Adv Clin Exp Med 2018;27:21–37. [PubMed: 29521040]

8). Stancker TG, Vieira SS, Serra AJ, do Nascimento Lima R, Dos Santos Feliciano R, Silva JA Jr., et al. Can photobiomodulation associated with implantation of mesenchymal adipose-derived stem cells attenuate the expression of MMPs and decrease degradation of type II collagen in an experimental model of osteoarthritis? Lasers Med Sci 2018;33:1073–1084. [PubMed: 29520686]

9). McDaniel K, Meng F, Wu N, Sato K, Venter J, Bernuzzi F, et al. Forkhead box A2 regulates biliary heterogeneity and senescence during cholestatic liver injury in micedouble dagger. Hepatology 2017;65:544–559. [PubMed: 27639079]

10). Glaser S, Meng F, Han Y, Onori P, Chow BK, Francis H, et al. Secretin stimulates biliary cell proliferation by regulating expression of microRNA 125b and microRNA let7a in mice. Gastroenterology 2014;146:1795–1808,e1712. [PubMed: 24583060]

11). McDaniel K, Huang L, Sato K, Wu N, Annable T, Zhou T, et al. The let-7/Lin28 axis regulates activation of hepatic stellate cells in alcoholic liver injury. J Biol Chem 2017;292:11336–11347. [PubMed: 28536261]

12). Hirsova P, Ibrahim SH, Verma VK, Morton LA, Shah VH, LaRusso NF, et al. Extracellular vesicles in liver pathobiology: Small particles with big impact. Hepatology 2016;64:2219–2233. [PubMed: 27628960]

13). Sato K, Meng F, Glaser S, Alpini G. Exosomes in liver pathology. J Hepatol 2016;65:213–221. [PubMed: 26988731]

14). Todorova D, Simoncini S, Lacroix R, Sabatier F, Dignat-George F. Extracellular vesicles in angiogenesis. Circ Res 2017;120:1658–1673. [PubMed: 28495996]

15). Morales-Kastresana A, Telford B, Musich TA, McKinnon K, Clayborne C, Braig Z, et al. Labeling extracellular vesicles for nanoscale flow cytometry. Sci Rep 2017;7:1878. [PubMed: 28500324]

16). Masyuk AI, Huang BQ, Ward CJ, Gradilone SA, Banales JM, Masyuk TV, et al. Biliary exosomes influence cholangiocyte regulatory mechanisms and proliferation through interaction with primary cilia. Am J Physiol Gastrointest Liver Physiol 2010;299:G990–G999. [PubMed: 20634433]

17). Sato K, Meng F, Venter J, Giang T, Glaser S, Alpini G. The role of the secretin/secretin receptor axis in inflammatory cholangiocyte communication via extracellular vesicles. Sci Rep 2017;7:11183. [PubMed: 28894209]

18). Matsuura K, De Giorgi V, Schechterly C, Wang RY, Farci P, Tanaka Y, et al. Circulating let-7 levels in plasma and extracellular vesicles correlate with hepatic fibrosis progression in chronic hepatitis C. Hepatology 2016;64:732–745. [PubMed: 27227815]

19). Arbelaiz A, Azkargorta M, Krawczyk M, Santos-Laso A, Lapitz A, Perugorria MJ, et al. Serum extracellular vesicles contain protein biomarkers for primary sclerosing cholangitis and cholangiocarcinoma. Hepatology 2017;66:1125–1143. [PubMed: 28555885]

20). Wu N, Meng F, Invernizzi P, Bernuzzi F, Venter J, Standeford H, et al. The secretin/secretin receptor axis modulates liver fibrosis through changes in transforming growth factor-beta1 biliary secretion in mice. Hepatology 2016;64:865–879. [PubMed: 27115285]

21). Falkowski O, An HJ, Ianus IA, Chiriboga L, Yee H, West AB, et al. Regeneration of hepatocyte 'buds' in cirrhosis from intrabiliary stem cells. J Hepatol 2003;39:357–364. [PubMed: 12927921]

22). Carpino G, Renzi A, Franchitto A, Cardinale V, Onori P, Reid L, et al. Stem/progenitor cell niches involved in hepatic and biliary regeneration. Stem Cells Int 2016;2016:3658013. [PubMed: 26880956]

23). Carpino G, Cardinale V, Onori P, Franchitto A, Berloco PB, Rossi M, et al. Biliary tree stem/progenitor cells in glands of extrahepatic and intraheptic bile ducts: an anatomical in situ study yielding evidence of maturational lineages. J Anat 2012;220:186–199. [PubMed: 22136171]

24). Haga H, Yan IK, Takahashi K, Matsuda A, Patel T. Extracellular vesicles from bone marrow-derived mesenchymal stem cells improve survival from lethal hepatic failure in mice. Stem Cells Transl Med 2017;6:1262–1272. [PubMed: 28213967]

25). Haga H, Yan IK, Borrelli DA, Matsuda A, Parasramka M, Shukla N, et al. Extracellular vesicles from bone marrow-derived mesenchymal stem cells protect against murine hepatic ischemia/reperfusion injury. Liver Transpl 2017;23:791–803. [PubMed: 28407355]

26). Chen L, Lu FB, Chen DZ, Wu JL, Hu ED, Xu LM, et al. BMSCs-derived miR-223-containing exosomes contribute to liver protection in experimental autoimmune hepatitis. Mol Immunol 2018;93:38–46. [PubMed: 29145157]

27). Murakami Y, Toyoda H, Tanahashi T, Tanaka J, Kumada T, Yoshioka Y, et al. Comprehensive miRNA expression analysis in peripheral blood can diagnose liver disease. PLoS One 2012;7:e48366. [PubMed: 23152743]

28). Cermelli S, Ruggieri A, Marrero JA, Ioannou GN, Beretta L. Circulating microRNAs in patients with chronic hepatitis C and non-alcoholic fatty liver disease. PLoS One 2011;6:e23937. [PubMed: 21886843]

29). Ustianenko D, Chiu HS, Treiber T, Weyn-Vanhentenryck SM, Treiber N, Meister G, et al. LIN28 selectively modulates a subclass of let-7 microRNAs. Mol Cell 2018;71:271–283.e5. [PubMed: 30029005]

30). Kumar M, Ahmad T, Sharma A, Mabalirajan U, Kulshreshtha A, Agrawal A, et al. Let-7 microRNA-mediated regulation of IL-13 and allergic airway inflammation. J Allergy Clin Immunol 2011;128:1077–1085,e1071-1010. [PubMed: 21616524]

31). Jiang LQ, Franck N, Egan B, Sjogren RJ, Katayama M, Duque-Guimaraes D, et al. Autocrine role of interleukin-13 on skeletal muscle glucose metabolism in type 2 diabetic patients involves microRNA let-7. Am J Physiol Endocrinol Metab 2013;305:E1359–E1366. [PubMed: 24105413]

32). Gieseck RL III, Ramalingam TR, Hart KM, Vannella KM, Cantu DA, Lu WY, et al. Interleukin-13 activates distinct cellular pathways leading to ductular reaction, steatosis, and fibrosis. Immunity 2016;45:145–158. [PubMed: 27421703]

33). Stedman C, Liddle C, Coulter S, Sonoda J, Alvarez JG, Evans RM, et al. Benefit of farnesoid X receptor inhibition in obstructive cholestasis. Proc Natl Acad Sci U S A 2006;103:11323–11328. [PubMed: 16844773]

34). Thomson J, Hargrove L, Kennedy L, Demieville J, Francis H. Cellular crosstalk during cholestatic liver injury. Liver Res 2017;1:26–33. [PubMed: 29552372]

35). Kennedy LL, Meng F, Venter JK, Zhou T, Karstens WA, Hargrove LA, et al. Knockout of microRNA-21 reduces biliary hyperplasia and liver fibrosis in cholestatic bile duct ligated mice. Lab Invest 2016;96:1256–1267. [PubMed: 27775690]

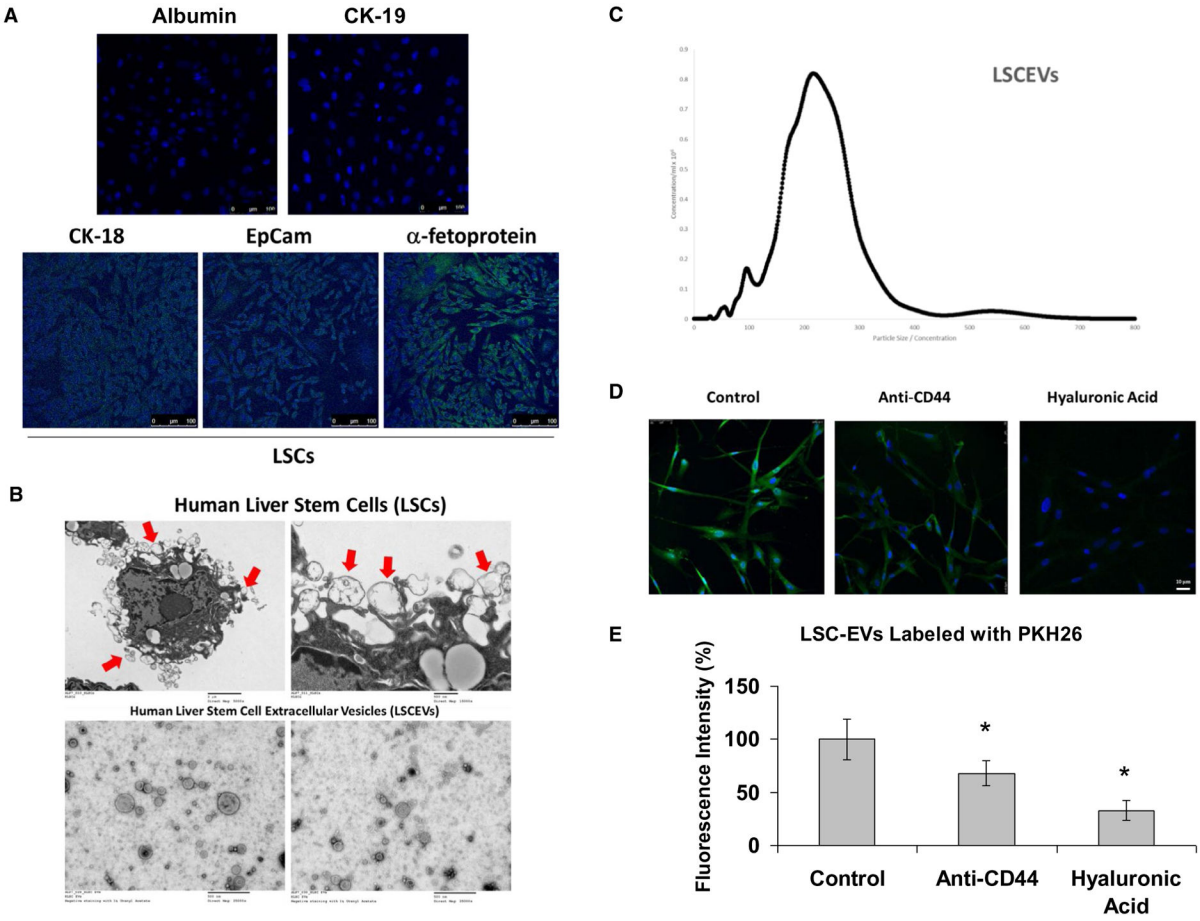

FIG. 1.

Characterization of LSCs and LSCEVs. (A) Immunocytochemistry was used for the detection of the presence of the liver progenitor cell markers (CK-18, EpCam, and alpha fetoprotein) in cultured LSCs. (B) TEM was used to image LSCs secreting EVs at magnification ×5,000 (upper left panel) and ×15,000 (upper right panel). EVs that are in the process of being secreted by LSCs are identified with red arrows. Isolated EVs were imaged with TEM at magnification ×25,000 (lower panels). (C) After LSCEV isolation, a NanoSight instrument was used to measure isolated EV size and abundance of the preparation. Data are plotted as particle size versus abundance. (D,E) Incorporation of LSCEVs in human H69 cholangiocyte cell line. Representative micrographs of internalization by H69 cells (30 minutes at 37°C) of EVs labeled with PKH26 green dye or preincubated with 100 μg/mL of sHA, or with 1 μg/mL of blocking monoclonal antibody against CD44 (D). Fluorescence intensity of PKH26 green dye was measured using NIH Image J software analysis of microphotographs of six randomly selected areas (E). Bar graphs are expressed as mean ± SEM of three independent experiments. $*P < 0.05$ relative to LSCEV control group. Abbreviation: sHA, soluble hyaluronic acid.

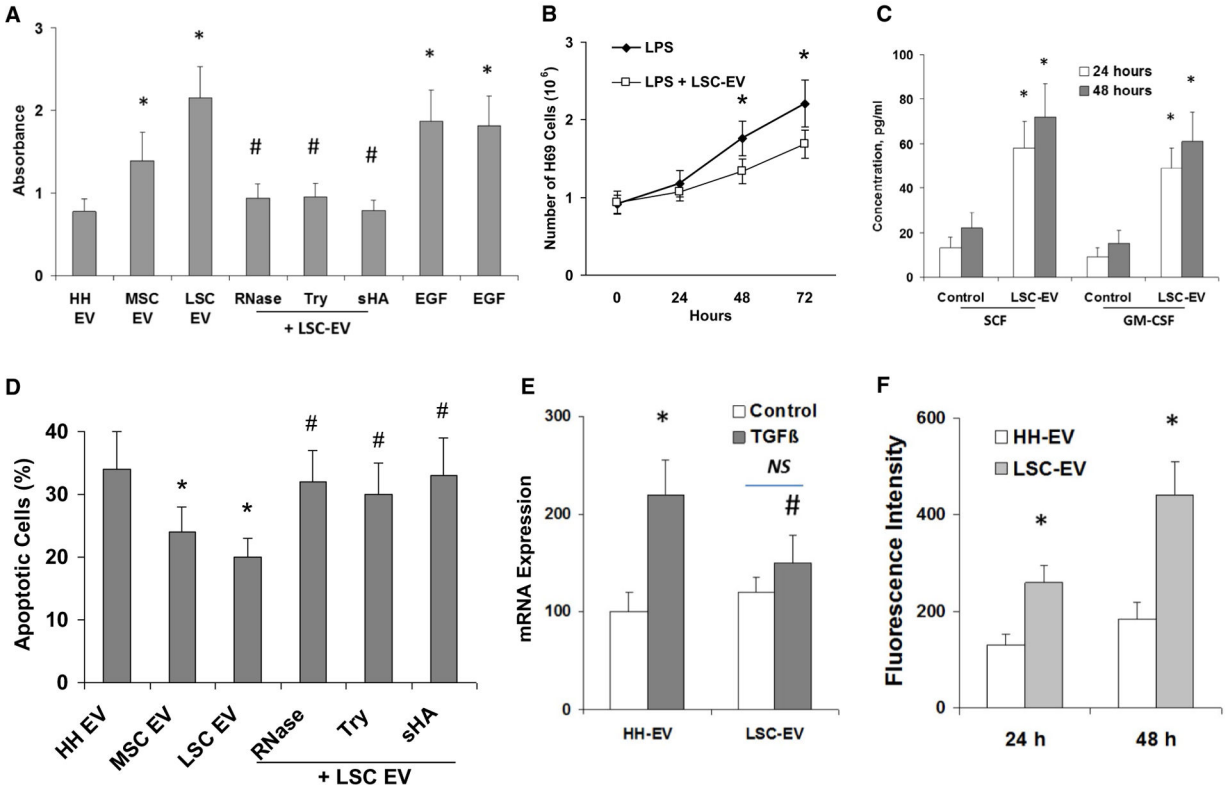

FIG. 2.

Regulation of proliferative, apoptotic, and fibrosis effects by LSCEVs in human cholangiocytes. (A) A bromodeoxyuridine (BrdU) cell proliferation assay kit (Colorimetric; Novus Biologicals, LLC, Centennial, CO) was used, and 10 μM BrdU was added to 4,000 cells/well (H69 cells) into 96-well plates and incubated for 48 hours in Dulbecco's modified Eagle's medium (DMEM) deprived of fetal bovine serum in the presence of normal HHEVs or human MSCEVs or human LSCEVs, with various treatments as indicated. Endothelial growth factor-induced (10 ng/mL) proliferation was also evaluated in H69 cells incubated with or without ribonuclease (RNase)-pretreated LSCEVs (30 μg/mL). The absorbance was measured at 450 nm using the iD5 Multi-Mode Microplate Reader from Molecular Devices (San Jose, CA). (B) LSCEV treatment also blocked LPS-induced cholangiocyte proliferation. In the presence of LPS, H69 cells exhibited a doubling time of 46 hours, whereas LSCEV-treated cells (30 μg/mL) exhibited a doubling time of approximately 67 hours ($P < 0.05$ at 48 hours and 72 hours control versus LSCEV-treated cells). Data are presented as the mean number of cells ± SEM from three independent experiments. (C) Release of stem cell factor and granulocyte-macrophage colony-stimulating factor by 1×10^5 H69 cells incubated for 24 hours or 48 hours with 30 μg/mL LSCEVs compared with H69 cells incubated with HHEVs (control). (D) The percentage of apoptotic cells after 48-hour TNF-α stimulation (100 ng/mL) was evaluated by the TUNEL (terminal deoxynucleotidyl transferase dUTP nick end labeling) assay. TNF-α-treated H69 cells were incubated with different kinds of EVs or RNase-treated LSCEVs, or LSCEVs pretreated with trypsin or 100 μg/mL of sHA. (E) Effect of LSCEVs on TGF-β-induced fibrosis marker α-SMA in H69 cholangiocytes. H69 cholangiocytes were treated with TGF-β (25 mM) in

the presence of EVs as indicated for 48 hours. Viable cells were collected, and the total RNA was isolated for real-time quantitative PCR analysis. (F) Effect of LSCEVs on TGF-β-inhibited senescence of human HSCs. HSCs were treated with EVs plus TGF-β (25 mM) for 48 hours. The cellular senescence index was measured by fluorescence intensity of β-gal cellular senescence assay. $^{*}P < 0.05$ relative to HHEV or respective controls. $^{\#}P < 0.05$ relative to LSCEV or TGF-β controls. Abbreviations: NS, not significant; sHA, soluble hyaluronic acid.

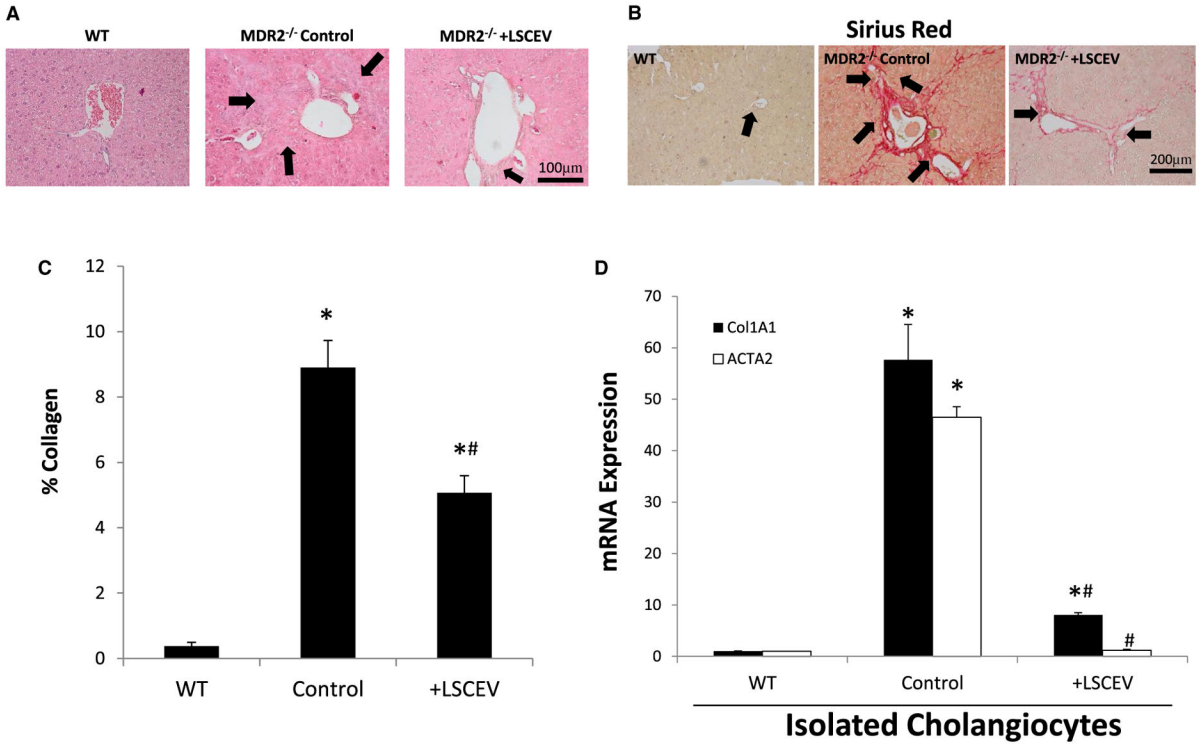

FIG. 3.

Analysis of inflammation and fibrosis in MDR2$^{-/-}$ mice treated with LSCEVs. (A) MDR2$^{-/-}$ mice were treated with LSCEVs or vehicle (phosphate-buffered saline) and compared with WT mice. Liver tissue samples from mice were evaluated with hematoxylin and eosin staining to evaluate structural anatomy of the liver. Black arrows indicate areas of inflammation in the liver. (B) Liver-tissue sections were stained with sirius Red, a marker of collagen. Arrows indicate areas of increased collagen deposition (red color). (C) Sirius red staining was quantified by dividing the area of red staining by the total area with ImageJ software and plotted as a bar graph ± SEM. *$P < 0.05$ versus WT; $^{\#}P < 0.05$ versus MDR2$^{-/-}$. (D) Real-time quantitative PCR was performed in isolated cholangiocytes for the fibrotic markers (Col1A1 and ACTA2) normalized to WT expression. Data are presented as mean ± SEM. *$P < 0.05$ versus WT; $^{\#}P < 0.05$ versus MDR2$^{-/-}$.

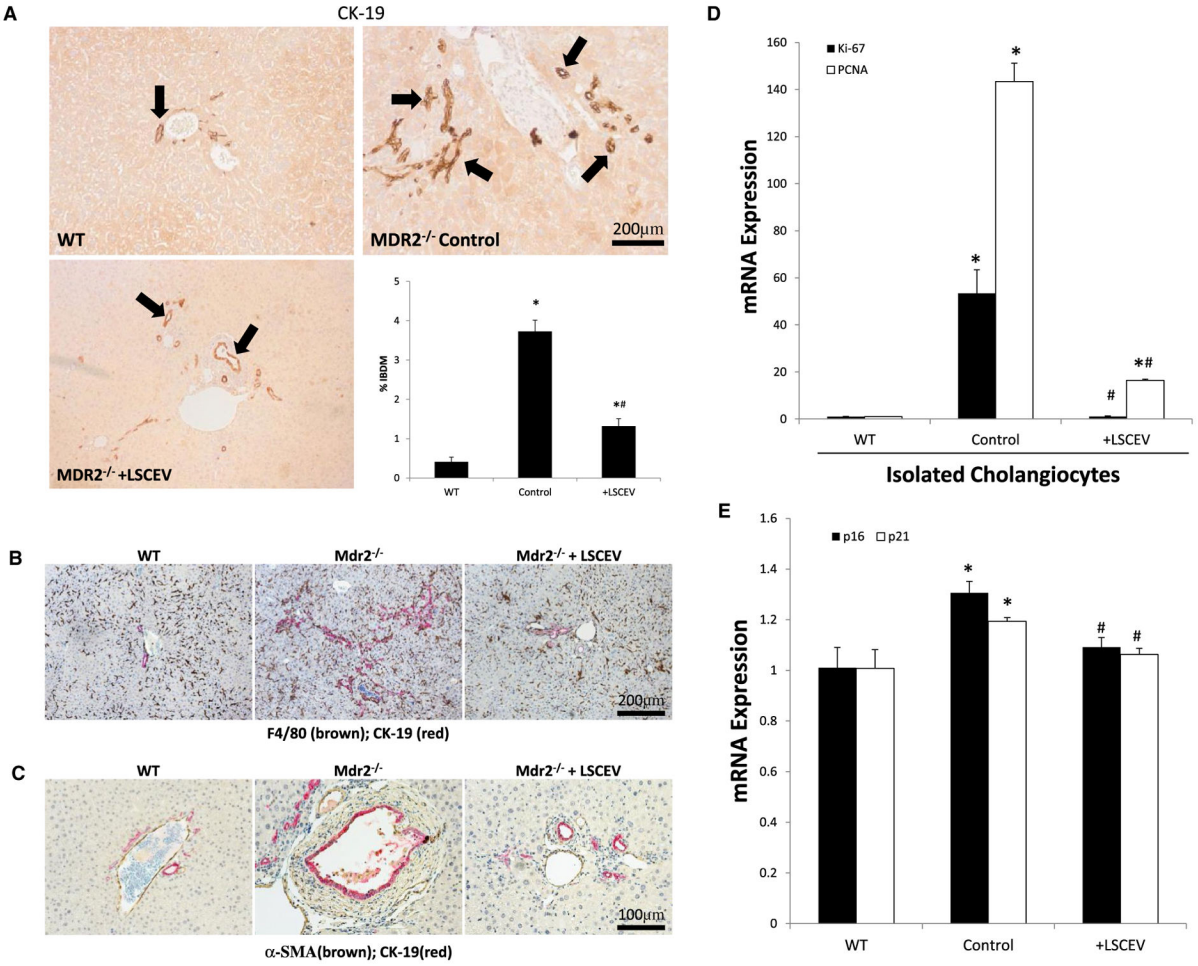

FIG. 4.

Evaluation of cholangiocyte proliferation and interactions with other cell types. (A) Liver tissue sections from WT, MDR2$^{-/-}$, and MDR2$^{-/-}$ plus LSCEVs were stained with CK-19, a marker of cholangiocytes, to evaluate biliary mass. Biliary mass was measured by quantifying the amount of positive staining by the total area. This quantification is displayed as mean percentage of biliary mass ± SEM. *$P < 0.05$ versus WT; $^{\#}P < 0.05$ versus MDR2$^{-/-}$. (B,C) Macrophage infiltration (marker F4/80) and liver fibrosis (marker α-SMA) around ductular reaction areas (marker CK-19) were detected in MDR2$^{-/-}$ mouse livers when compared with WT control by double-staining immunohistochemistry analysis. Multiple antigen labeling in the same tissue section was done using the VECTASTAIN systems (Vector Laboratories, Inc., Burlingame, CA). Specific enzyme substrates were incubated in sections to develop contrasting optimal color (F4/80/α-SMA, brown; CK-19, red). The representative images from four separate experiments are displayed. (D) Cholangiocyte proliferation was measured with real-time quantitative PCR for the proliferation markers PCNA and Ki-67. Data are normalized to WT and presented as mean ± SEM. *$P < 0.05$ versus WT; $^{\#}P < 0.05$ versus MDR2$^{-/-}$. (E) Total liver senescence was measured by real-time quantitative PCR for the senescence markers p16 and p21. Data are shown as mean ± SEM. *$P < 0.05$ versus WT; $^{\#}P < 0.05$ versus MDR2$^{-/-}$.

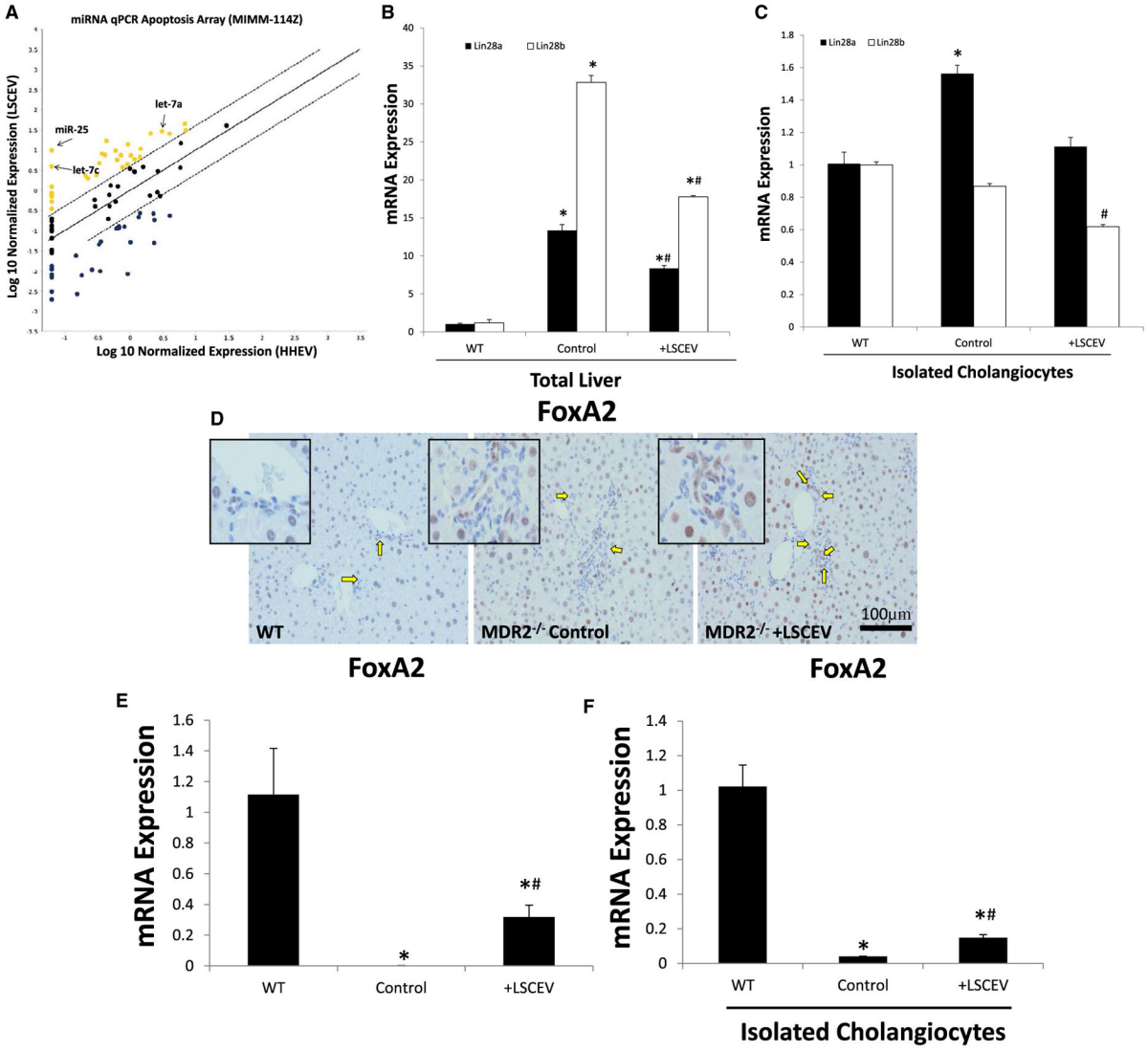

FIG. 5.

Identification of LSCEV content and downstream pathways. (A) To identify miRNA contents of LSCEVs, an apoptosis microRNA real-time quantitative PCR array was used to evaluate levels of miRNAs compared to HHEVs. Data points above the standard error of the mean were considered elevated in LSCEVs compared to HHEVs. miRNAs involved in liver disease and repair were identified and labeled. (B,C) To evaluate the downstream target of let-7, Lin28, real-time quantitative PCR was evaluated in total liver (B) and isolated cholangiocytes (C) for both Lin28A and Lin28B. Data are presented as mean ± SEM. $^{*}P < 0.05$ versus WT; $^{\#}P < 0.05$ versus MDR2$^{-/-}$. (D) FoxA2, a marker of repair, and a downstream target of the let-7 pathway, was measured in liver sections with immunohistochemistry. Positive cells and stained brown and positive cholangiocytes are indicated by yellow arrows. FoxA2 expression levels were measured with real-time quantitative PCR in total liver (E) and isolated cholangiocytes (F). Data are expressed as mean ± SEM. $^{*}P < 0.05$ versus WT; $^{\#}P < 0.05$ versus MDR2$^{-/-}$.

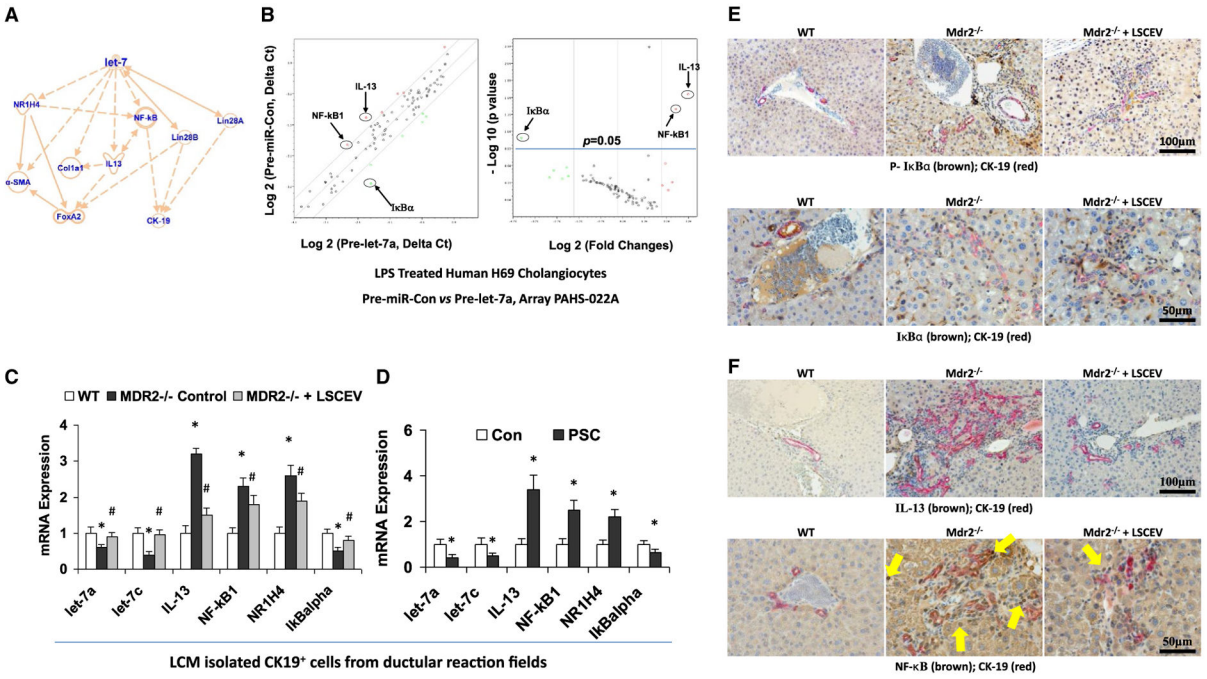

FIG. 6.

Let-7 associated anti-inflammation and antifibrosis signaling mechanisms in LSCEV-treated H69 cells and MDR2 $^{-/-}$ mice liver. (A) IPA based on LSEC treatment in MDR2 $^{-/-}$ mice and miRNA PCR array discoveries showed that let-7 may target IL-13/NR1H4/NF-κB and subsequently alter the ductular reaction/inflammation/fibrosis signaling pathways. (B) The expression levels of key mediators of NF-κB signaling pathway are altered in Pre-let-7a-transfected H69 human cholangiocytes after LPS stimulation relative to Pre-miRNA-Con. Relative gene-expression profile between Pre-let-7a-transfected H69 cells after LPS stimulation versus Pre-miRNA-Con is shown. The expression of a panel of diverse inflammation-associated genes was evaluated by real-time PCR assay using the Human Chemokines & Receptors PCR Array (PAHS-022; SABiosciences Corp., Valencia, CA), which was selected based on IPA with a focus on the NF-κB signaling–associated gene list. Gene expression relative to GAPDH was plotted as the volcano plots, depicting the relative expression levels (Log10) for selected genes in Pre-miR-Con versus Pre-let-7a (left panel). The relative expression levels and *P* values for each gene in the related samples were also plotted against each other in the scatterplot (right panel). The key mediators of NF-κB signaling pathway, NF-κB1, IkBα and IL-13, are the most altered genes in Pre-let-7a-treated H69 cells after LPS stimulation. Data represent the mean from three separate experiments. (C) Total RNA was isolated from CK-19-positive cells collected from ductular reaction fields in control and LSCEV-treated MDR2$^{-/-}$ mice liver sections by LCM, and Taqman real-time PCR assay and real-time quantitative PCR assay were carried out to detect let-7a and let-7c expressions, along with the mRNA expressions of inflammation/fibrosis markers (IL-13, NF-κB1, and NR1H4). LSCEV treatment significantly increased the biliary expression of let-7 in ductular reaction fields in MDR2$^{-/-}$ mice, along with the significant reductions of inflammation/fibrosis markers IL-13, NF-κB1, and NR1H4 when compared with the relative controls. $^{*}P < 0.05$ relative to WT controls; $^{\#}P < 0.05$ relative to MDR2$^{-/-}$

controls. (D) Total RNA was collected from cholangiocytes isolated from the ductular reaction areas of liver sections from PSC patients by laser capture microdissection compared with healthy controls, and real-time quantitative PCR analysis was performed as described in the Materials and Methods. The miRNA and mRNA expression of let-7 (let-7a and let-7c) and inflammation/fibrosis markers (IL-13, NF-κB1, and NR1H4) were increased, whereas IκBα was decreased, in the cholangiocytes from ductular reaction fields from PSC patients' liver compared with healthy controls. *$P < 0.05$ relative to normal controls. (E) Phosphorylation of IkBα (top panel) and degradation of IkBα (bottom panel) were detected in ductular reaction fields by double-staining immunohistochemistry analysis using cholangiocytes specific marker CK-19 plus phosphorylation or total IkBα antibodies in LSCEV-treated MDR2$^{-/-}$ mice liver relative to controls. (F) IL-13 expression and NF-κB nuclear translocation detected ductular reaction fields (marker: CK-19) in LSCEV-treated MDR2$^{-/-}$ mice liver when compared with MDR2$^{-/-}$ and WT controls by double-staining immunohistochemistry analysis. Multiple antigen labeling was performed in the same tissue section using the VECTASTAIN systems. Specific enzyme substrates were incubated in sections to develop contrasting optimal color (IL-13/NF-κB, brown; CK-19, red). The representative images from four separate experiments are displayed. Original magnifications: ×100 and ×50. Abbreviation: GAPDH, glyceraldehyde 3-phosphate dehydrogenase.

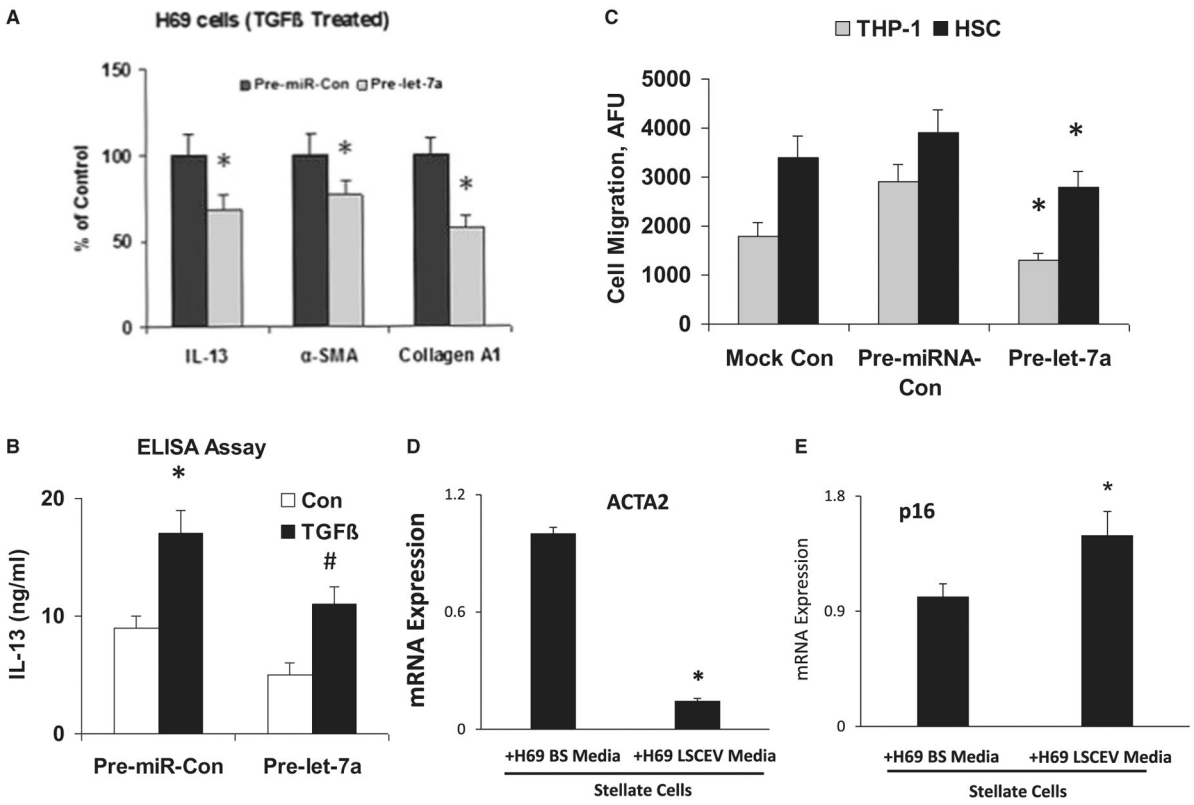

FIG. 7.

Let-7/LSCEV-mediated anti-inflammatory and antifibrotic interactions between cholangiocyte and human macrophages/human hepatic stellate cells. (A,B) Pre-let-7a treatment inhibits TGF-β-stimulated cholangiocytes and suppresses the migration of THP-1 cells. (A) Effects of Pre-let-7a on the mRNA expression of inflammation/fibrosis markers in H69 human cholangiocytes. H69 cells were transfected with 100 nM Pre-miRNA-Con or 100 nM Pre-let-7a. After incubation in DMEM with 1% FCS, the cells were treated with TGF-β (25 mM) for 48 hours. Cellular RNAs were isolated, and the expressions of IL-13, α-SMA, and Col1A1 mRNA levels were examined by real-time quantitative PCR. GAPDH mRNA was used for normalization. (B) Effects of Pre-let-7a on the expression of cytokine IL-13 at the protein level. Conditioned medium was collected from TGF-β-stimulated H69 cells (25 mM for 48 hours), and enzyme-linked immunosorbent assay was performed to assess IL-13 expression. (C) Migrations of the human monocyte cell line THP-1 and human HSCs were suppressed by conditioned media from Pre-let-7a-transfected H69 cells. A total of 5×10^5 THP-1 cells or 5×10^3 human HSCs were placed in the upper chamber, and conditioned medium from TGF-β-stimulated H69 cells transfected with Pre-miR-Con or Pre-let-7a was added to the lower chamber. After 3 hours of incubation, THP-1 cells or HSCs that migrated toward the lower chamber were detected by fluorescent dye. Relative fluorescence units (AFUs) are indicated (versus 1% FCS). All results are shown as mean ± SEM. A minimum of three replicates were performed for each set of experiments to compile the data as presented. $*P < 0.05$ relative to Pre-miR-Con group. To evaluate the interactions among LSCs, cholangiocytes and HSCs, H69 human cholangiocytes were incubated with LSCEVs for 48 hours; the media was then changed to new media for 24 hours. The H69

media was removed and used to treat stellate cells for 48 hours. The stellate cells were then used to extract mRNA and perform real-time quantitative PCR for the fibrosis marker, ACTA2 (D), and the senescence marker, p16 (E). Abbreviations: ELISA, enzyme-linked immunosorbent assay; GAPDH, glyceraldehyde 3-phosphate dehydrogenase.

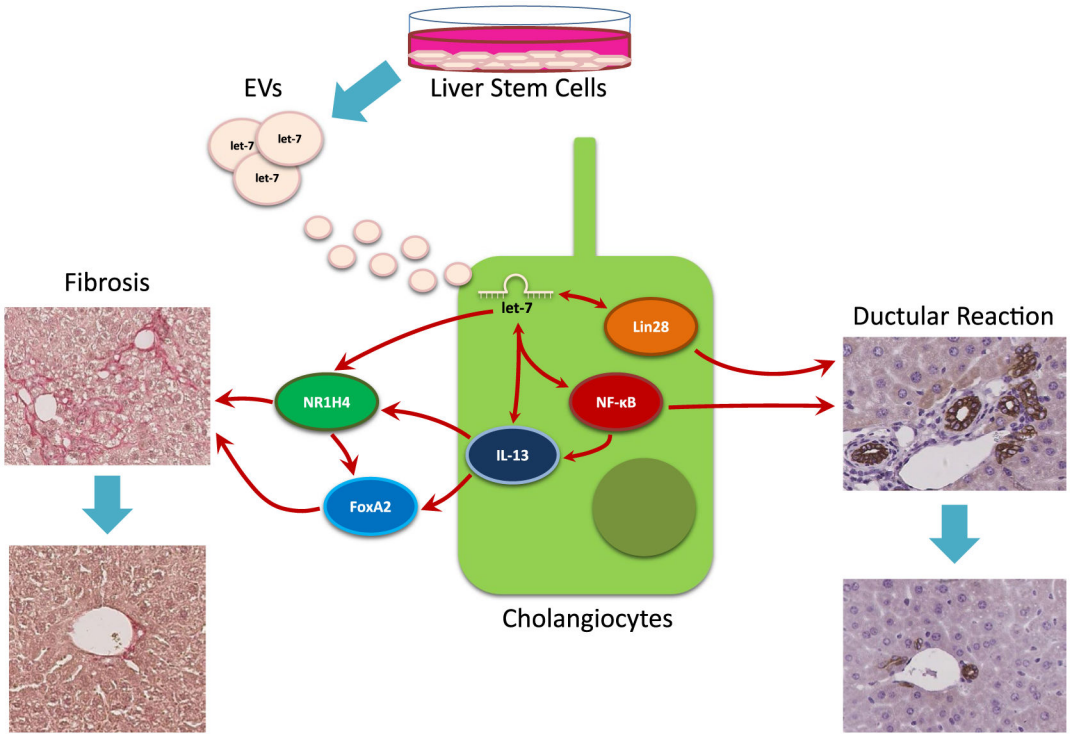

FIG. 8.

Summary of the Interactions between LSCEVs containing let-7 and cholangiocytes and subsequent inhibition of ductular reaction and liver fibrosis. LSCs release LSCEVs, which are received by cholangiocytes, causing increased let-7 in cholangiocytes. This allows let-7 to inhibit Lin28 and influence IL-13 and NF-κB, which reduces the ductular reaction. Let-7 and IL-13 are also able to influence the levels of NR1H4 and FoxA2, which decreases liver fibrosis.